Astronomy & Astrophysics

A new *Herschel* view of the young star T54: not a transitional disk?[★]

L. Matrà[1,2], B. Merín[1], C. Alves de Oliveira[1], N. Huélamo[3], A. Kóspál[4], N. L. J. Cox[5], Á. Ribas[1,3], E. Puga[1], R. Vavrek[1], P. Royer[5], T. Prusti[4], G. L. Pilbratt[4], and P. André[6]

[1] Herschel Science Centre, ESAC-ESA, PO Box 78, Villanueva de la Cañada, 28691 Madrid, Spain
   e-mail: lmatra@sciops.esa.int
[2] School of Physics, Trinity College Dublin, Dublin 2, Ireland
[3] Centro de Astrobiología, INTA-CSIC, PO Box - Apdo. de correos 78, Villanueva de la Cañada, 28691 Madrid, Spain
[4] Research and Scientific Support Department, ESTEC-ESA, PO Box 299, 2200 AG Noordwijk, The Netherlands
[5] Instituut voor Sterrenkunde, K.U. Leuven, Celestijnenlaan 200D, 3001 Leuven, Belgium
[6] Laboratoire AIM Paris – Saclay, CEA/DSM – CNRS – Université Paris Diderot, IRFU, Service d'Astrophysique, Centre d'Études de Saclay, Orme des Merisiers, 91191 Gif-sur-Yvette, France

Received 28 September 2012 / Accepted 25 October 2012

ABSTRACT

Context. Observations of transitional disks give us an understanding of the formation of planets and planetary systems such as our own. But care must be taken in identifying such sources: the higher spatial resolution of the *Herschel* Space Observatory provides a new view of the origin of the far-infrared and submillimeter excesses observed.
Aims. We review the nature of previously known transitional disks in the Chamaeleon I star-forming region with *Herschel* data.
Methods. We analyze *Herschel* PACS and SPIRE images of the young star T54, together with ancillary images. We also analyze its spectral energy distribution and indications from optical and mid-infrared spectroscopy.
Results. We detect extended emission in the PACS 70 μm image $\sim$6″ off source at a position angle of 196° from T54. The emission detected at longer wavelengths (PACS 100, 160, SPIRE 250 and 350 μm) is also offset from the position of the star. This suggests that the excess observed in the far-infrared part of the SED is not fully associated with T54.
Conclusions. *Herschel* images show that the far-infrared excess seen in T54 is not due to a transitional disk but to extended emission southwest of the source. The object still shows point-like and now downscaled excess at mid-infrared wavelengths, but its origin cannot be constrained without higher spatial resolution data. However, different indications point towards an evolved disk or extended unresolved emission close to the source.

Key words. stars: formation – stars: pre-main sequence – protoplanetary disks – circumstellar matter – stars: individual: HM Anon

1. Introduction

Transitional disks (TDs) are circumstellar disks that exhibit inner clearings or gaps induced by physical processes, such as photoevaporation, grain growth, and dynamical interactions with stellar companions or candidate planets. This causes a wide range of spectral energy distribution (SED) properties to be observed (Williams & Cieza 2011, and references therein). Disks are identified as transitional if they have no or small near-infrared (near-IR) excess, steep slopes in the mid-IR, and large far-IR excesses (e.g. Merín et al. 2010). However, the different definitions used sometimes make their identification problematic. In fact, similar SEDs can be reproduced by a number of environments, including background objects and nebulosity in the source surroundings, which can contaminate and bias the sample of known transitional disks. In addition to this, asymptotic giant branch stars and classical Be stars can easily be mistaken for TDs with a significant flux deficit at all wavelengths and $\alpha_{excess} < 0$ (e.g. Cieza et al. 2010), and SEDs of edge-on protoplanetary disks can look like those of TDs with a sharp rise in the mid-IR (Merín et al. 2010). See review from Williams & Cieza (2011) and references therein for a more detailed description.

To accomplish a more thorough characterization of this class of young objects, there is a need to examine their fluxes at far-IR wavelengths. *Herschel*, with its improved spatial resolution, can greatly serve the purpose of ruling out sources affected by contamination. In the Chamaeleon I star-forming region (Cha I), the young object T54 (also NAME HM Anon) is one of eight candidate transitional disks (Manoj et al. 2011). The star has been reported as a spectral type G8 (Luhman 2007), weak-lined T Tauri (WTTS; Nguyen et al. 2012), with a visual extinction of 1.78 mag and luminosity of 4.1 $L_\odot$ (Kim et al. 2009). T54 is a known subarcsecond binary (Ghez et al. 1997; Lafrenière et al. 2008). The companion is located at a projected separation of 0″.247 (43 AU) and position angle (PA) of 246.5°. Resolved optical spectra by Nguyen et al. (2012) suggest that the optical luminosity of the system is dominated by the primary component, although we cannot rule out that the IR excess at the position of T54 discussed later partially originated in the secondary.

2. Observations

2.1. Herschel

The Chamaeleon I region was observed by the *Herschel* Space Observatory (Pilbratt et al. 2010) as part of the Gould Belt Survey (André et al. 2010). A detailed description of the observations can be found in Winston et al. (2012). Observations were

---

taken using the PACS (Poglitsch et al. 2010) and SPIRE (Griffin et al. 2010) instruments in parallel-mode (obsids 1342213178 and 1342213179; 22 Jan. 2011) for the 70 and 160 μm PACS, and the 250 and 350 μm SPIRE bands. Additional PACS observations were obtained in the 100 μm band (obsids 1342224782, 1342224783, 1342225003, and 1342225004; dates 27 Jul. 2011 and 1 Aug. 2011). The data were reduced using HIPE (Ott 2010) version 8.2.0 and processed using the Scanamorphos (Roussel 2012) software v14 for PACS, and the Scan Map Destriper pipeline in HIPE for SPIRE. The astrometry of the PACS images was refined using 2MASS PSC positions of nearby point sources through the Astrometrical Calibration tool in the Aladin v7 software (Bonnarel et al. 2000).

Photometry was extracted using the HIPE *annularSkyAperturePhotometry* task, which performs aperture photometry with background subtraction. For PACS, aperture corrections were applied and photometric errors estimated as specified in the PACS Point-Source Flux Calibration Technical Note from April 2011. For SPIRE, the same was applied using apertures and corrections from Sect. 5.7.1.2 of the SPIRE Data Reduction Guide, with a conservative uncertainty of ±10%.

2.2. Ancillary data

Ancillary images were retrieved to check, through visual inspection, the possible presence of counterparts for the extended emission around T54 discovered by *Herschel*. The FORS 1 Hα image (PROG ID 075.C-0809(A), 26 Jul. 2005) was obtained from the ESO Archive, while 2MASS All-Sky Release Survey images (25 Jan. 2000) were obtained from the 2MASS Interactive Image Service. IRAC (AOR key 20014592, 16 May 2007) and MIPS (AOR key 5706752, 24 Dec. 2009) Post BCD images were obtained from the *Spitzer* Heritage Archive. The IRS spectrum (AOR key 12695552) was extracted from the *Spitzer* Heritage Archive and reduced with SPICE v2.5.0. The short low slit (5.2−14.5 μm) included only T54, while the long low slit (14.0−38.0 μm) included both T54 and 2MASS J11124076-7722378. While the PSFs slightly overlap, the sources are resolved enough that an uncontaminated spectrum of T54 could be extracted by using a narrow aperture.

3. Results

Figure 1 presents *Herschel* and ancillary images centered at RA$_{2000}$ = 11^{h}12^{m}42^{s}029 Dec$_{2000}$ = −77°22′28′′58 to display the source and its surroundings. T54 is clearly detected as a point source (top-left cross in Fig. 1) at all optical, near-, and mid-IR wavelengths. Extended emission is discovered in the PACS 70 μm image at a distance of ~6′′ and PA of 196° from T54. In the 100 μm image we observe emission in an elongated shape whose photocenter is offset from the star. This off-source emission observed is unique to T54: it was not found in any *Herschel* images of the other known transitional disks in the Chamaeleon I and II regions (Ribas et al., in prep.). In 160, 250, and 350 μm images, we also observe extended emission centered off-source. However, we note that the increased PSF size makes it impossible to rule out a possible contribution from the nearby point source 2MASS J11124076-7722378 (bottom-right cross in Fig. 1) at PA 203° and distance of 16′′ from T54. Inspection of 2MASS color-color and color-magnitude diagrams shows very extreme colors compared to young Cha I members, indicating that this is likely an unrelated background object. No detection was obtained in SPIRE 500 μm, owing to the presence of strong emission from the environment of the Cha I cloud.

Table 1. *Herschel* photometry.

Instrument	Wavelength (μm)	Flux (Jy)	Aperture radius ($''$)
PACS	70 (star-only)	0.23 ± 0.03	4
PACS	70 (offset em.-only)	0.22 ± 0.03	4
PACS	70 (star+offset em.)	0.48 ± 0.03	8
PACS	100	0.61 ± 0.02	8
PACS	160	1.10 ± 0.11	22
SPIRE	250	0.49 ± 0.05	22
SPIRE	350	0.24 ± 0.02	30

Table 1 presents *Herschel* aperture corrected fluxes, together with the apertures used. Background sky annuli with radii of 25′′ and 40′′ for all PACS images, and 60′′ and 90′′ for SPIRE were subtracted.

Figure 2 presents the SED of the object updated with the values from Table 1. After applying a NEXTGEN stellar model (Hauschildt et al. 1999; Allard et al. 2000) for spectral type G8, we observe that the SED shows no or very little infrared excess at wavelengths ≲10 μm. The mid-IR excess at wavelengths up to 70 μm is attributed to the unresolved circumstellar environment originated in the star position, as confirmed by the point-like emission in the *Spitzer* MIPS 24 μm image. At longer wavelengths we cannot attribute the measured fluxes to the star, but mostly to the nearby extended emission and possible additional contamination from 2MASS J11124076-7722378. As a result, a significant part of the far-infrared excess seen in the SED of T54 (about half at 70 μm, likely more at increasing wavelengths) does not originate in the star position, but comes from nearby extended emission resolved by *Herschel*.

If we assume that the remaining downscaled excess arises from thermal emission from dust grains, a single-temperature blackbody fit yields a dust temperature of approximately 94 K. We estimate the luminosity of the star by integrating the photospheric fluxes as ~3.66 $L_\odot$, and the luminosity of the dust from integration under the mid-IR blackbody curve. This leads to a fractional luminosity value of $L_{IR}/L_* = 0.005$.

We finally use the pre-main sequence tracks from Palla & Stahler (1999) in the census of Chamaeleon I by Luhman (2004) to estimate the age and mass of T54. We find that the system is between 3 and 10 Myr old, with a mass of approximately 1.5 $M_\odot$. This is consistent with the age spread in the Chamaeleon I region found by Luhman (2004), in which objects of different mass have an age ranging between 1 and 10 Myr. However, they also find a median age of ~2 Myr, implying that T54 has a more evolved nature than do most sources in the cluster.

4. Discussion

In this section we discuss previous information about T54 in the context of the new *Herschel* data. The main result is the discovery of extended emission contaminating the far-infrared part of the SED (discussed in Sect. 4.1), which scales down significantly the total excess attributed to the source. This potentially changes the nature of T54: in Sect. 4.2 we draw a comparison with similar objects, and then conclude in Sect. 4.3 by considering the new characteristics of the system if a disk is still present.

4.1. Far-infrared extended emission

In the PACS 70 μm image we clearly resolve extended emission with its flux peaking at a projected distance of 1040 AU and PA of 196° from the star. At longer wavelengths this emission
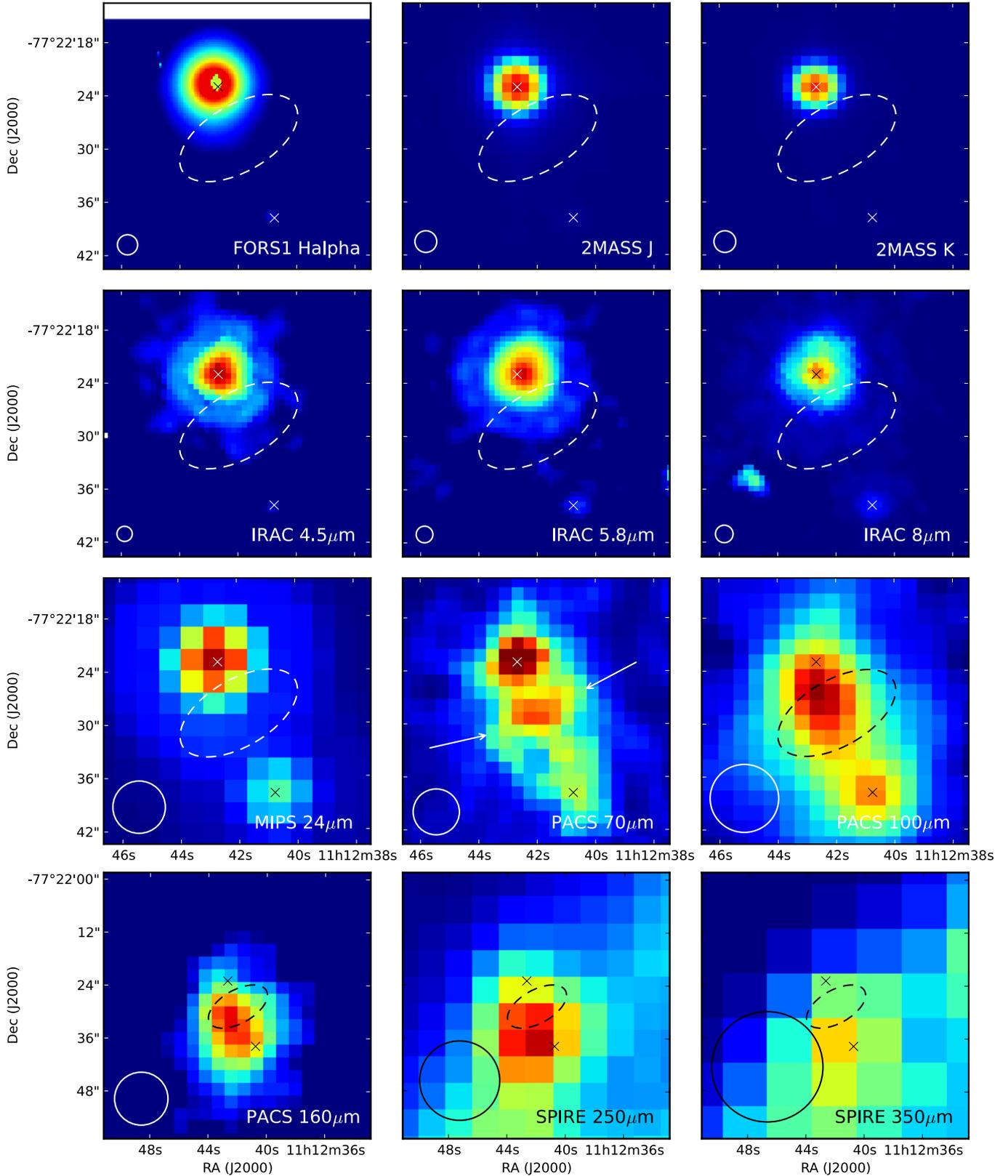
Fig. 1. Images of T54 at different wavelengths. North is up, east is left. The *bottom* row images show a region twice as large as the other ones. The diameter of the circles in the bottom left of each image represents the FWHM of the PSF for the different observations. The northern cross is centered on the position of T54 from the 2MASS *Point Source Catalog*, while the southern one corresponds to the position of 2MASS J11124076-7722378. Arrows indicate the location of extended emission as detected at 70 μm, and the dashed ellipse represents the same in all other images. Unlabeled objects represent artifacts.
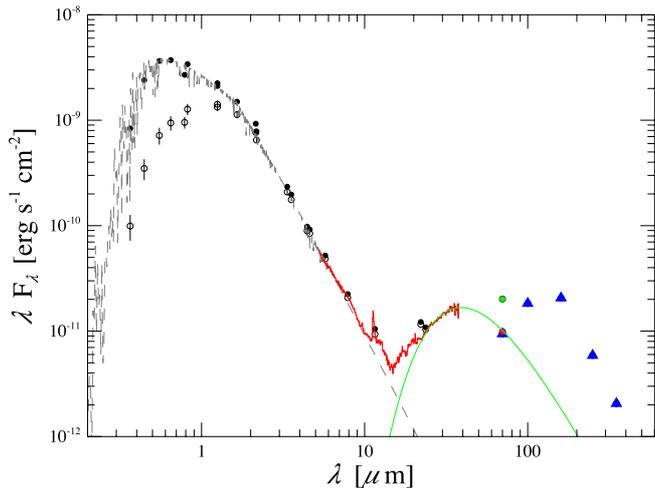
Fig. 2. Spectral energy distribution of T54. Open circles are observed optical, DENIS, 2MASS, WISE PRC, *Spitzer* IRAC, and MIPS 24 μm fluxes from the literature. Solid black circles are the fluxes dereddened with an A_V of 1.78 mag using the law from Weingartner & Draine (2001). The red line is the *Spitzer* IRS spectrum. The dashed line is the G8 NEXTGEN stellar model that best fits the optical photometry. At 70 μm, PACS fluxes displayed are from the star only (red solid circle), from the extended emission only (blue solid triangle) and from both (green solid circle). Longer wavelength *Herschel* flux values, not from the star position, are shown as blue solid triangles. The green solid line represents a $T = 94$ K blackbody curve fit to the mid-IR fluxes.

is not resolved, but most of the flux comes from its position. Presence of nebulous emission has been reported in the literature. Both Gauvin & Strom (1992) and Spangler et al. (2001) report the emission from the source being extended at IRAS and ISO wavelengths. Furthermore, the presence of a reflection nebula (referred to as GN11.11.2 or BRAN341E) was reported in a study by Brand et al. (1986) and its position is consistent with the emission discovered. We conclude that about half of the excess at 70 μm is not to be associated with a transitional disk at the star position but to extended emission offset from it, likely associated with a small reflection nebula. At longer *Herschel* wavelengths, the latter is not resolved, but most of the excess seems to originate in it, and not in the position of the system. These results cause a reduction of the total excess flux attributed to T54 and thus modify the view we had of its nature.

4.2. Comparison with other objects

The system is classified as nonaccreting due to its Hα line in absorption (Nguyen et al. 2012; Feigelson & Kriss 1989; Walter 1992), with the latter, however, indicating substantial filling in of the line, as in the case of the young object DoAr 21 (Jensen et al. 2009), discussed further below. This contrasts with all but two of the rest of the transitional disks in Chamaeleon I (Manoj et al. 2011). On the other hand, we note that Kim et al. (2009) report that the source is accreting from analysis of its U-band flux. High Hα and U-band variability has been reported in objects of similar nature, such as T Cha (Schisano et al. 2009) and DoAr21 (Jensen et al. 2009), even on a timescale of days. In addition to this, flaring activity in T54 has been suggested in the X-ray study by Feigelson et al. (1993) as explaining the significant increase in flux between the *ROSAT* and the previous *Einstein* observations (Feigelson & Kriss 1989). This again enhances the similarity with DoAr 21, for which Jensen et al. (2009) suggests that flares could account for the U-band excess and variability observed. In

summary, most references point towards a nonaccreting stellar environment, but no conclusions can be drawn without further spectral observations.

T54 also presents polycyclic aromatic hydrocarbon (PAH) emission at 11.3 μm, which is undetected in the majority of disks around T Tauri stars (Geers et al. 2006). In this context, it is useful to compare T54 to the case of DoAr 21, since the latter is similarly a late spectral type with PAH features and lack of silicates. Interestingly, Jensen et al. (2009) obtained narrow-band images centered on the 11.3 μm feature and found a partial arc or ring of dust at a projected distance of 134 AU from the source. Even in the case of T54, it is therefore possible that the PAH emission originates in an extended area and is not associated with a circumstellar disk.

We also compare the X-ray properties of T54 to those of DoAr 21, and analyze how these can influence the presence of PAH emission. In the case of T54, Feigelson et al. (1993) report considerable X-ray luminosity ($\log(L_X) = 30.5$), which is not as extreme as the value for DoAr 21 ($\log(L_X) \simeq 32$, Jensen et al. 2009). Jensen et al. (2009) suggest that strong X-ray emission could be responsible for exciting the PAHs. However, a more recent study by Siebenmorgen & Krügel (2010) shows that X-rays destroy PAH molecules efficiently at all distances. This would make the detection of PAHs around such strong X-ray emitters very unlikely, and therefore cannot explain the 11.3 μm feature observed.

Furthermore, T54 does not display a 10 μm silicate feature even though transitional disks commonly show it (Manoj et al. 2011). A broad study of disks with inner holes by Merín et al. (2010) presents only three objects lacking this feature, namely DoAr 21, SSTc2d J18285808+0017243, and Sz 84, which interestingly also have SEDs very similar to T54, and PAH features in two of them. These three out of a sample of 35 disks were all classified as probable extended sources and therefore dubious transitional disks. However, in the case of T54, we cannot exclude the presence of a disk with a very clean inner hole, such as T25 in Cha I (Kim et al. 2009) and IRAS 04125+2902 in Taurus (Furlan et al. 2011). Therefore, the lack of the 10 μm silicate feature also raises doubts about the disk nature of the source.

4.3. Concluding remarks

If the downscaled excess, however, originated in a disk, this would have an evolved nature. In fact, its fractional luminosity of 0.005 is consistent with the definition of a debris disk from Wyatt (2008) ($L_{IR}/L_* < 10^{-2}$), and our age estimate sets the system among the most evolutionary advanced in the Cha I region. Using Eq. (3) in Wyatt (2008), we obtain a disk radius of 16.8 AU, which is smaller than the 43 AU binary separation (Lafrenière et al. 2008) and would make T54 an interesting case of an evolved disk around a single binary component. However, no conclusions can be drawn without observations at higher spatial resolution, which are needed to better constrain the nature of this system.

References

Allard, F., Hauschildt, P. H., & Schweitzer, A. 2000, ApJ, 539, 366
André, P., Men'shchikov, A., Bontemps, S., et al. 2010, A&A, 518, L102
Bonnarel, F., Fernique, P., Bienaymé, O., et al. 2000, A&AS, 143, 33
Brand, J., Blitz, L., & Wouterloot, J. G. A. 1986, A&AS, 65, 537
Cieza, L. A., Schreiber, M. R., Romero, G. A., et al. 2010, ApJ, 712, 925
Feigelson, E. D., & Kriss, G. A. 1989, ApJ, 338, 262
Feigelson, E. D., Casanova, S., Montmerle, T., & Guibert, J. 1993, ApJ, 416, 623
Furlan, E., Luhman, K. L., Espaillat, C., et al. 2011, ApJS, 195, 3
Gauvin, L. S., & Strom, K. M. 1992, ApJ, 385, 217
Geers, V. C., Augereau, J.-C., Pontoppidan, K. M., et al. 2006, A&A, 459, 545
Ghez, A. M., McCarthy, D. W., Patience, J. L., & Beck, T. L. 1997, ApJ, 481, 378
Griffin, M. J., Abergel, A., Abreu, A., et al. 2010, A&A, 518, L3
Hauschildt, P. H., Allard, F., Ferguson, J., Baron, E., & Alexander, D. R. 1999, ApJ, 525, 871
Jensen, E. L. N., Cohen, D. H., & Gagné, M. 2009, ApJ, 703, 252

Kim, K. H., Watson, D. M., Manoj, P., et al. 2009, ApJ, 700, 1017
Lafrenière, D., Jayawardhana, R., Brandeker, A., Ahmic, M., & van Kerkwijk, M. H. 2008, ApJ, 683, 844
Luhman, K. L. 2004, ApJ, 602, 816
Luhman, K. L. 2007, ApJS, 173, 104
Manoj, P., Kim, K. H., Furlan, E., et al. 2011, ApJS, 193, 11
Merín, B., Brown, J. M., Oliveira, I., et al. 2010, ApJ, 718, 1200
Nguyen, D. C., Brandeker, A., van Kerkwijk, M. H., & Jayawardhana, R. 2012, ApJ, 749, 94
Ott, S. 2010, in Astronomical Data Analysis Software and Systems XIX, eds. Y. Mizumoto, K.-I. Morita, & M. Ohishi, ASP Conf. Ser., 434, 139
Palla, F., & Stahler, S. W. 1999, ApJ, 525, 772
Pilbratt, G. L., Riedinger, J. R., Passvogel, T., et al. 2010, A&A, 518, L1
Poglitsch, A., Waelkens, C., Geis, N., et al. 2010, A&A, 518, L2
Roussel, H. 2012 [arXiv:1205.2576]
Schisano, E., Covino, E., Alcalá, J. M., et al. 2009, A&A, 501, 1013
Siebenmorgen, R., & Krügel, E. 2010, A&A, 511, A6
Spangler, C., Sargent, A. I., Silverstone, M. D., Becklin, E. E., & Zuckerman, B. 2001, ApJ, 555, 932
Walter, F. M. 1992, AJ, 104, 758
Weingartner, J. C., & Draine, B. T. 2001, ApJ, 548, 296
Williams, J. P., & Cieza, L. A. 2011, ARA&A, 49, 67
Winston, E., Cox, N. L. J., Prusti, T., et al. 2012, A&A, 545, A145
Wyatt, M. C. 2008, ARA&A, 46, 339